Structure and Thermodynamics of $H^+(H_2O)_n$ (n = 9, 21, 40) Clusters between 0 and 300 K. A Monte Carlo Study

Marcus Svanberg and Jan B. C. Pettersson*

Department of Chemistry, Physical Chemistry, and School of Environmental Sciences, Göteborg University, S-412 96 Göteborg, Sweden

Received: November 3, 1997

We present a Monte Carlo study of protonated water clusters, $H^+(H_2O)_n$, with size n = 9, 21, and 40, and neutral clusters, $(H_2O)_{20}$, in the temperature range 0 to 300 K. We study the structural differences between the solidlike and liquidlike phases, using an empirical polarizable water model. The transition between these two phases is particularly distinct in $H^+(H_2O)_{21}$, which attains the dodecahedral cage configuration at temperatures up to 150 K, a structure that does not survive above 170 K. The results support the idea that the "magic number" behavior of $H^+(H_2O)_{21}$ is restricted to temperatures below the melting point. We estimate the melting temperatures for $H^+(H_2O)_9$, $H^+(H_2O)_{21}$, and $(H_2O)_{20}$ as predicted by the model to be 130, 160, and 160 K, respectively. The melting process in the protonated clusters thus appears to be governed mainly by water−water interactions.

Introduction

The field of cluster science represents a systematic way of investigating how properties of aggregates of atoms or molecules change as the size of the system grows from only a few constituents to the bulk limit. Neutral and charged water clusters are interesting not only from a fundamental point of view, but their properties are important in a number of disciplines, including aqueous solvation, biochemistry, aerosol, and atmospheric sciences.[1,2] Although previous theoretical work on protonated water clusters has almost exclusively focused on the most stable structures, together with a few studies of the room-temperature behavior, we investigate here the full range of temperatures and focus on the transition from solidlike to liquidlike structures. We have chosen clusters containing between 9 and 40 water molecules to cover a size range where the properties of this transition may be significantly different.

The transition between solidlike and liquidlike regimes in clusters has previously attracted considerable attention.[3,4] As the size reaches the macroscopic limit, the familiar melting phase transition will be recovered, but in small aggregates the penalty in (free) energy associated with forming an interface may prevent the two phases from coexisting simultaneously.[5] The absence of long-range order also modifies the bulk picture, but it has been shown by a number of molecular dynamics (MD) and Monte Carlo (MC) computer simulations that small argon clusters exhibit two distinct phases for certain sizes, for example Ar_7 and Ar_{13}.[3] Wales and Ohmine[6] also found transitions between solidlike and liquidlike phases from MD studies on $(H_2O)_8$ and $(H_2O)_{20}$ clusters. They furthermore illustrated the importance of starting from a low energy structure, ideally the global energy minimum, for obtaining reliable thermodynamic results. It has been shown that even for a relatively small cluster, such as $(H_2O)_8$, there exists a large number of local energy minima,[7,8] and to our knowledge no efficient procedure to locate the global minimum exists for clusters of typically 20 molecules.[9] So, even if the calculations are restricted to a relatively simple (analytic) interaction potential, which may be more or less accurate, one must therefore rely on approximate methods for locating the lowest local minimum.

Many experimental studies of protonated water clusters, or proton hydrates, have found a "magic number" behavior of the $H^+(H_2O)_{21}$ cluster[10−15]; that is, it is more abundant in the mass spectra than the neighboring sizes. It has been shown to contain 10 free (non-hydrogen bonded) hydrogens.[16] Other mass spectrometric measurements have reported on enhanced stability of the $NH_4^+(H_2O)_{20}$,[17] $OH^-(H_2O)_{20}$,[18] and $Cs^+(H_2O)_{20}$[19] clusters. Castleman and co-workers[19] have used a flow reactor technique to study water clusters containing different alkali metal cations. Although the $K^+(H_2O)_{20}$ and $Cs^+(H_2O)_{20}$ clusters show clear magic number behavior, $Li^+(H_2O)_{20}$ and $Rb^+(H_2O)_{20}$ are somewhat weaker and $Na^+(H_2O)_{20}$ does not appear to be a magic number. Because magic number behavior must be connected with an increased stability of a certain cluster size, it has been proposed that pentagonal dodecahedral cages surround the ions,[16,19] assuming a central H_3O^+ ion in the $H^+(H_2O)_{21}$ cluster, which would presumably give especially stable structures.

The experimental findings have prompted a number of simulations[2,12,20−23] of $H^+(H_2O)_n$ clusters. These studies have focused on sizes around n = 21, addressing the origin of the magic number behavior based on analytical interaction potentials. Because of the uncertain accuracy of the potentials, however, final conclusions about the structure are difficult to draw. The more recent articles have reported various geometries as candidates for the most stable structure. David[21] applied the Stillinger-David polarization model and a simple minimization procedure and observed migration of the excess proton, originally in the center of a filled dodecahedron, to a surface water molecule. Kozack and Jordan[23−25] devized an empirical water−

* Author to whom correspondence should be addressed. Tel: +46.31.772 28 28. Fax: +46.31.772 31 07. E-mail: janp@phc.chalmers.se.

S1089-5639(98)00052-8 CCC: $15.00
Published on Web 02/12/1998

water potential including molecular polarizability,[24] together with a proton model,[25] and subsequently used it in a study of $H^+(H_2O)_n$ clusters with $n = 20-22$.[23] As the lowest $H^+(H_2O)_{21}$ minima they found a dodecahedral and two disordered structures with interior hydronium-like ions, which were all close in energy. For the $H^+(H_2O)_{20}$ cluster, a surface structure was reported as the minimum. Kelterbaum and Kochanski[2,22] have performed room-temperature MC simulations of $H_3O^+(H_2O)_N$ clusters, with N up to 28, using pairwise water−water and water−hydronium potentials combined with a three-body water−ion−water potential. They conclude that for optimized geometries, the hydronium ion in the model prefers surface structures instead of being located in the interior of a dodecahedron. Smith and Dang[26] performed a detailed investigation of low-energy cage structures for $Cs^+(H_2O)_{20}$ clusters and concluded that the minimum configuration had not only five-membered rings, as in the pentagonal dodecahedron, but also four- and six-membered rings. However, the polarizable model used in the simulation still predicted $Cs^+(H_2O)_{20}$ to be especially stable in the solidlike regime. These findings illustrate clearly the possibility of alternative cage structures being responsible for the observed magic number behavior of the ion-doped $(H_2O)_{20}$ clusters.

High-level ab initio calculations on protonated water clusters are mainly restricted to the minimum energy structures of relatively small systems such as $H_5O_2^+$[27,28] and $H_9O_4^+$.[28] Larger systems require more approximate methods, as for example the density functional treatment of $H_9O_4^+$[29] or the semiempirical quantum mechanical study of clusters up to $H^+(H_2O)_{14}$.[30] Khan[31] also used a semiempirical quantum mechanical method to study clathrate structures of $(H_2O)_{20}$, $H^+(H_2O)_{20}$, and $H^+(H_2O)_{21}$ clusters. After optimization of $H^+(H_2O)_{21}$, it was found that the excess proton, initially placed in the center, had migrated to the surface leaving a water molecule within the cage. Laasonen and Klein[32] studied $(H_2O)_{20}$ and $H^+(H_2O)_{21}$ clusters using gradient-corrected density functional theory. Both predefined symmetric geometries as well as others generated by simulated annealing with an SPC potential were optimized by steepest decent. A disordered structure, which had an hydronium-like unit on the surface, was found to be essentially degenerate in energy with one where the hydronium unit was encaged within a (distorted) pentagonal dodecahedron. The authors point out that also the disordered surface structure has 10 free hydrogens, thus matching the experimental findings of Castleman.[16] An analysis of the charge distribution revealed that within a sphere of radius 1.4 Å, the net charge of this unit was $+0.8\ e$; thus supporting the H_3O^+ interpretation of the structure. The development of ab initio MD techniques, such as the Car-Parrinello[33] and BO-MD methods,[34] has also enabled dynamic studies without the use of conventional interaction potentials. Both pure bulk water[35] as well as the solvation and transport of hydronium and hydroxyl ions in liquid water[36] have been simulated with ab initio MD. When studying the system with an excess proton, Tuckerman et al.[36] could identify an $H_9O_4^+$ unit in 60% of the configurations and an $H_5O_2^+$ complex, where the proton resided midway between two oxygen atoms, in the remainder of the trajectory. As a result of proton transfer, the solvation complex continuously fluctuates between these two structures. Although this type of simulations impressively provides information on the electronic structure of a system containing as many as tens of molecules, also at temperatures above 0 K, the calculation of the electronic distribution at each time-step obviously sets restrictions on the accessible simulation time, and applications to, for example, the phase transition region are currently intractable.

In this article, we use MC simulations to study the behavior of intermediately sized protonated water clusters between 0 and 300 K, applying the empirical polarizable model of Kozack and Jordan.[24,25] Neutral water clusters were also examined to investigate what effect the ion had on the charged clusters, and to assess the performance of the interaction potential. Apart from the fundamental interest in water clusters, the present study is also motivated by the need to better understand the properties of proton hydrates observed in the mesopause at altitudes of 82−89 km under cold conditions.[37,38] It has been proposed that these hydrates may serve as condensation nuclei in the formation of noctilucent clouds.[39] These positively charged clusters may recombine with free electrons whereby a large amount of energy is released. Depending on how this energy is distributed within the cluster, it may either partially survive or fragmentize completely, which will affect the possibility of subsequent condensation.[40] The energy distribution process will in turn depend on the structure of the clusters, which is controlled by environmental parameters, such as the temperature and water partial pressure. In the simulations, we therefore pay particular attention to the range of possible locations of the charged unit within the clusters, because we expect it to be a key parameter controlling the degree of fragmentation that follows the dissociative recombination. We regard this work as an investigation of realistic and reasonably accurate structures of neutral and protonated water clusters, and in particular the perturbations induced by thermal motion. The preceding discussion has clearly pointed out difficulties in locating the most stable structures of these clusters, and our primary interest is not to elaborate further on this matter. A detailed study of the neutralization/fragmentation of proton hydrates is currently in progress.

The remainder of the article is organized as follows: In the next section we describe the simulation model together with the MC procedure and method of analysis. The following section presents the results that are discussed and related to previous work. The last section sums up the main conclusions of this article.

Model and Calculations

Canonical MC simulations have been applied to $H^+(H_2O)_n$ ($n = 9$, 21, 40) and $(H_2O)_{20}$ clusters according to the Metropolis scheme[41] at temperatures between 0 and 300 K. We have used the empirical polarizable rigid water model developed by Kozack and Jordan[24] (hereafter denoted by KJ) for the H_2O-H_2O interaction. In the model, a water molecule has its gas-phase geometry with O−H bond length 0.957 Å and H−O−H bond angle 104.5°. Each molecule carries the partial charge q on each H site, $2q$ on the O site, and $-4q$ on a δ site located 0.138 Å from the O site along the H−O−H bisector, where q equals 0.6228 e. Two water molecules interact electrostatically and via a Lennard-Jones 12−6 potential, with parameters $\epsilon_{LJ} = 18.23$ meV and $\sigma_{LJ} = 3.17$ Å, where the intermolecular separation is measured between the δ sites. In addition, many-body interactions are modeled by placing a point scalar polarizability on the δ site, with a molecular polarizability volume $\alpha = 1.47$ Å^3. The electric field, **E**, at each δ site, caused by the surrounding charges and dipoles, induces a point dipole, **p**, according to:

$$\mathbf{p} = \alpha\mathbf{E} \tag{1}$$

Self-consistent dipoles[42] were obtained by iteration, until the polarization energy changed by <0.1 meV during one iteration.

The KJ water model has been found to account well for gas-phase and dimer properties, and a comparison with ab initio data for the trimer, tetramer, and pentamer showed reasonable agreement.[24] The experimental binding energy of three different polymorphs of ice was also successfully reproduced, although the model gives a density somewhat too low. For liquid water at 300 K, the major deficiencies are a binding energy that is 17% too high and pair correlation functions that show too little structure compared with experimental data. Although *effective* pair-potentials in general predict these properties better for liquid water,[43] we put more confidence in the performance of the KJ model concerning small clusters, especially at low temperatures, because it was optimized for a description of these systems. As a comparison, we have also applied the simple point charge (SPC) model[44] to the neutral $(H_2O)_{20}$ cluster.

To describe the ionic unit in the charged clusters, we have used the proton model of Kozack and Jordan[25] in which the proton carries a single point charge equal to $+e$. The proton also interacts with a water molecule via a hard-core potential of the form (C_{HC}/r_{HC}),[9] where $C_{HC} = 1.277$ eV$^{1/9}$ Å and r_{HC} is the distance between the proton and the δ site. In ref 25, interatomic distances in small clusters as well as binding energies compared well with ab initio results and experimental data, a conclusion that also applies when considering recent literature data.[45] Because of the strong binding energy of small $H_3O^+(H_2O)_N$ clusters (~1 eV per water molecule for N up to three[45]), we expect the explicit inclusion of many-body interactions to be important. Kozack and Jordan[25] also tested models in which the charged unit was modeled as an H_3O^+ ion,[25] but the resulting binding energies were less accurate than those of the proton model. Although the approximation of nondissociating water molecules does not permit charge transfer by the "structural diffusion mechanism"[36,46] or proton relay, we are concerned here with equilibrium properties that are less dependent on dynamic features of the system.

To prevent evaporation at elevated temperatures, the cluster was surrounded by a spherical r^{-12}-potential.[47,48] The sphere radius was set to 8, 6, 10, and 17 Å for $(H_2O)_{20}$, $H^+(H_2O)_9$, $H^+(H_2O)_{21}$, and $H^+(H_2O)_{40}$, respectively, and the average cluster-sphere energy was always lower than a few millielectronvolts. We have used several approaches to find as low minima as possible, including simulated annealing,[49] quenching, generation of pre-defined structures, or a combination of the three methods. Quenching was performed by running the cluster at a (high) temperature, and then at regular intervals setting the temperature to 100 K and decreasing it to 0 K linearly during typically 10^4 MC steps.

Because displacement of a single molecule requires all dipoles to be updated, we defined an MC step as translation and rotation of all molecules followed by acceptance/rejection.[41] The maximum displacement was typically 0.01 Å, and each (Euler angle) rotation 0.5% of its full range, adjusted to give an acceptance ratio close to 0.5. To search configuration space more efficiently, we also tried an approach where the proton and the two closest water molecules were subject to smaller displacements than the rest of the system. Because no significant improvements were observed, this technique was abandoned. For the low-temperature, solidlike clusters, as well as those close to the melting point, we always started from the lowest energy configuration and then ran a number of equilibration MC steps. In the subsequent production runs, configurations were analyzed and the potential energy, E_p, Lindemann index, δ_L, radius of gyration and radial distribution functions were calculated. The length of these runs are collected in Table 1. The Lindemann index, or relative root-mean-square bond length fluctuations, is defined as[3,50]:

TABLE 1: Number of Million Monte Carlo Steps in the Simulations

T, K	$(H_2O)_{20}$ (SPC)	$(H_2O)_{20}$ (KJ)	$H^+(H_2O)_9$	$H^+(H_2O)_{21}$	$H^+(H_2O)_{40}$
50	20	7	8	8	2
100	20	5	8	8	2
120	20	10	80		
140	40	40	80		
150			80	32	10
160	20	40	80		
170				24	
180	20	30	40	24	
200	20	40	40	24	
220		20		16	
250	10	20	50	16	10
300			50	16	10

$$\delta_L = \frac{2}{n(n-1)} \sum_{i<j} \frac{\sqrt{\langle r_{ij}^2 \rangle - \langle r_{ij} \rangle^2}}{\langle r_{ij} \rangle} \qquad (2)$$

where r_{ij} is the center of mass (CM) distance between molecule i and j, and the sum includes all H_2O-H_2O pairs. Lindemann's criterion for melting is $\delta_L \geq 0.1$, and it has proven to be a sensitive indicator of the melting transition in water[6,50] and rare gas[3,4] clusters. In MD simulations on chalcogen hexafluoride clusters, however, Bartell and co-workers[51] found less definite indications of melting from a Lindemann analysis and concluded that a threshold value of 0.08−0.09 was more appropriate for the systems under investigation. The three radii of gyration, K_i, are defined as $(I_i/M)^{1/2}$, where I_i is one of the three principal moments of inertia and M is the total cluster mass. The (geometric) average radius of gyration, K, is given by $(K_1K_2K_3)^{1/3}$. In ref 52, this index was found to give a good description of the geometrical changes accompanying the melting transition in icosahedral palladium clusters.

Results and Discussion

As a reference to the structural and thermodynamic characteristics of the protonated clusters, we have compared the KJ and SPC models for a neutral $(H_2O)_{20}$ cluster. The lowest energy structures of $(H_2O)_{20}$ have recently attracted considerable attention.[6,7,32,53] In agreement with the results in refs 6 and 53, we find that the SPC minimum is a pentagonal prism structure. For the KJ model on the other hand, simulated annealing during 25×10^6 steps gave a lower minimum for a cage-like structure with seven free hydrogens, as shown in Figure 1. Although a pentagonal prism with slightly different H-bonding than in ref 6 was only 0.04 eV higher in energy, we note that a pentagonal dodecahedron is as much as 0.19 eV above the cage-like structure. These findings are consistent with the conclusions of Berkowitz and co-workers[53] that polarizable models prefer cage-like structures to a larger extent than pair potentials. The structure also appears to be quite similar to the compact lowest energy structures with either seven or eight free hydrogens, obtained in the density functional study by Laasonen and Klein.[32] The appearance of these disordered structures as candidates for the global minimum also reinforces the idea that the different minimum structures can only be regarded as approximations to the absolute minimum. The resulting binding energies for all clusters are collected in Table 2.

In Figure 2 we compare Lindemann indices and average potential energies for the $(H_2O)_{20}$ clusters, using the KJ and

Figure 1. Lowest energy structure found for the $(H_2O)_{20}$ cluster modeled by the KJ potential. Both covalent and hydrogen bonds are indicated.

TABLE 2: Total Binding Energies E_b of the Neutral and Protonated Water Clusters, Defined as Negative Values of the Lowest Potential Energies[a]

cluster	E_b, eV	$<E_b>$, eV molecule^{-1} [b]	H bonds	method
$(H_2O)_{20}$ (SPC)	9.20	0.460	34	predefined
$(H_2O)_{20}$ (KJ)	8.87	0.444	33	annealed
$H^+(H_2O)_9$	13.55	0.690	11	quenched
$H^+(H_2O)_{21}$	19.94	0.600	33	predefined
$H^+(H_2O)_{40}$	30.03	0.567	68	annealed + quenched

[a] The number of hydrogen bonds and method of generation is also indicated. [b] Average binding energy *per water molecule*; for the protonated water clusters, the binding energy of the isolated $H^+(H_2O)$ complex (7.343 eV) was subtracted from E_b.

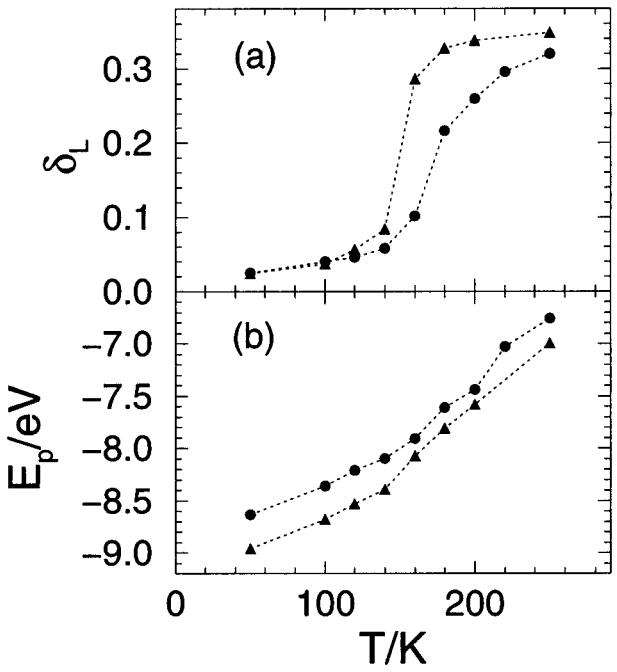

Figure 2. Lindemann index (δ_L) and potential energy (E_p) as a function of temperature for the $(H_2O)_{20}$ clusters, described by the (●) KJ and (▲) SPC models.

SPC water models. In the following we will estimate the melting temperature, T_m, by interpolating δ_L to 0.1. The two models then predict T_m(KJ) ≈ 160 K and T_m(SPC) ≈ 140 K. Both values compare well with the MD results from Ohmine and co-workers, where a model of the "TIPS" type (T4) gave $T_m \approx 160$ K for a $(H_2O)_{20}$ cluster,[6] and with $T_m \approx 180$ K obtained for a $(H_2O)_{108}$ SPC cluster.[50] The data are also consistent with the experimentally estimated freezing temperatures of 180 ± 20 K[54] and 200 K,[55] which were deduced from electron diffraction measurements in supersonic molecular beams with clusters containing a few thousand molecules. The phase behavior of a particular cluster depends on its underlying potential energy surface (PES) and in particular the free energy barrier that separates low-energy, solidlike configurations from high-energy, liquidlike states.[3−5,48,56] For $(H_2O)_8$, the melting temperature has been shown to depend sensitively on the H_2O-H_2O PES, yielding variations as large as 80−90 K.[6,48] In view of the differences of the KJ and SPC models, the melting temperatures agree quite well.

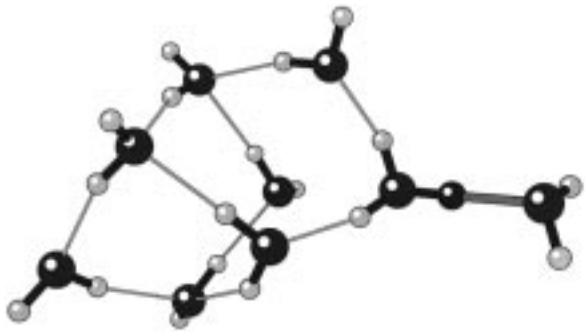

Figure 3. Lowest energy structure found for the $H^+(H_2O)_9$ cluster. Both covalent and hydrogen bonds are indicated and the proton is blackened.

At both low and high temperatures, $E_p(T)$ (or kinetic energy as a function of total energy in the microcanonical ensemble) varies approximately linearly, as seen in Figure 2b, and the system displays only solidlike or liquidlike behavior.[3,4,56] At intermediate temperatures, referred to as the transition region, the cluster may be found in both states. Bixon and Jortner[56] applied model partition functions and, in agreement with results from simulations,[3,4] they showed that if a cluster exhibits a sufficiently large energy gap in the spectrum of its local energy mimima, a well-defined phase transition occurs. Apart from the dependency on the energy spectrum, the width of the transition region was also shown to be larger in the canonical than in the microcanonical ensemble due to larger energy fluctuations. Judging from both δ_L and E_p in Figure 2, the width appears to be larger for the KJ model, although the high-temperature data are somewhat noisy. The melting process is initiated by a passage over a potential barrier, which may occur very rarely at low temperatures, and it is therefore a stochastic process. Although there is always a finite possibility that the solidlike clusters will eventually escape from that phase, the length of the runs at temperatures close to the melting point (Table 1) renders that possibility unlikely.

We will now turn our attention to the properties of the protonated water clusters. Although $H^+(H_2O)_9$ and $H^+(H_2O)_{21}$ are sufficiently small to exhibit properties that may change irregularly with cluster size, we would expect $H^+(H_2O)_{40}$ to be in a size range where a more smooth variation is obtained. For clusters larger than $H^+(H_2O)_2$, the excess proton in the KJ model attaches strongly to a specific water molecule with a short bond length of about 1.0−1.1 Å,[23] and we can identify this as an H_3O^+ unit. Because this complex has an asymmetric charge distribution, adding another water molecule will give a strongly interacting $H_5O_2^+$ unit (in the form $H_2O-H^+-OH_2$), which will also be present in larger clusters. For $H^+(H_2O)_9$, we obtain a binding energy of 13.55 eV, as seen in Table 2. Figure 3 shows

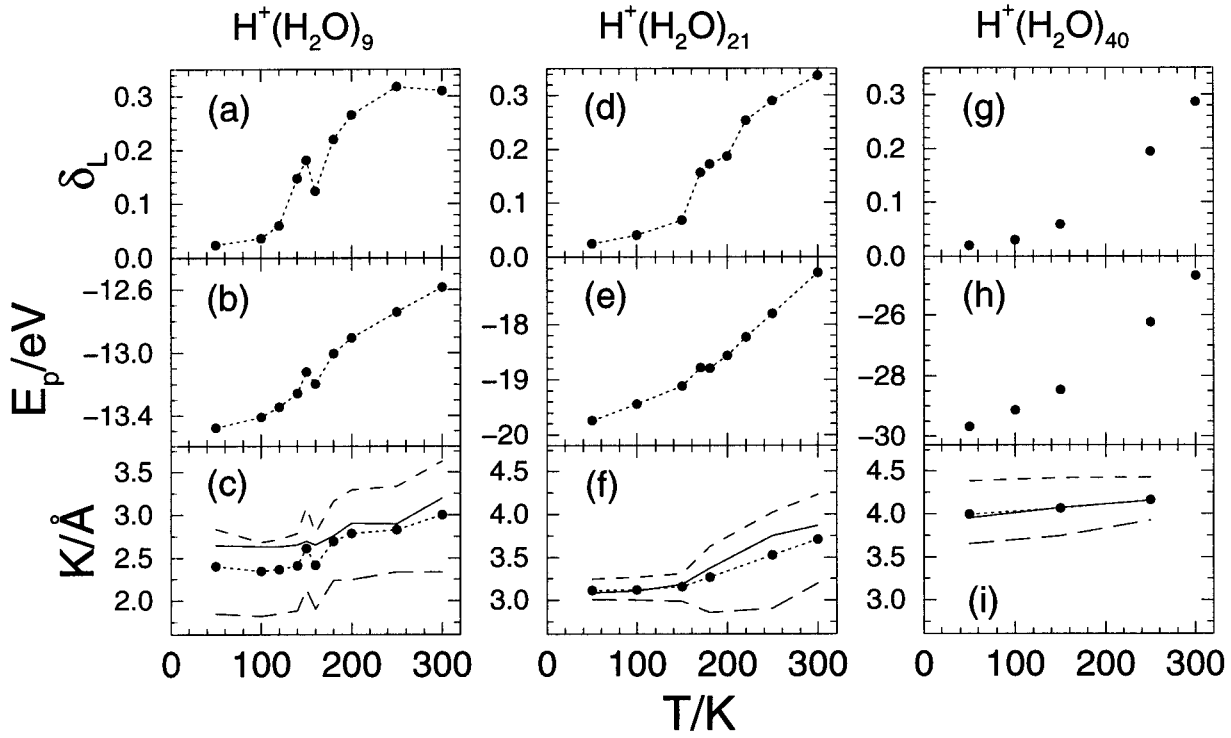

Figure 4. Temperature dependence of $H^+(H_2O)_9$ (panels a−c), $H^+(H_2O)_{21}$ (panels d−f), and $H^+(H_2O)_{40}$ (panels g−i). The upper row panels show the Lindemann index (δ_L), the middle row shows the potential energy (E_p), and the lower row shows average radius of gyration (K). The three principal radii of gyration K_1 (- - -), K_2 (—), and K_3 (— —) are also given in the lower row panels.

its structure, where all but one water molecule (being part of the $H_5O_2^+$ unit) reside on the same side of the H_3O^+ unit. This H-bonded network contains one four-membered and two five-membered rings. The benefit of attaining this configuration, instead of having more water molecules close to the proton, is an increase in the number of hydrogen bonds. Also, for smaller clusters like $H^+(H_2O)_{4-8}$, the KJ model prefers to have all but one water molecule on one side of the ionic unit.

Figure 4a−c shows the temperature dependence of the Lindemann index, potential energy, and radii of gyration for the $H^+(H_2O)_9$ cluster. From Figure 4a we estimate the melting temperature to be ∼130 K. Evidently, the transition region is quite broad as seen from the nonlinear portion of the E_p curve at intermediate temperatures in Figure 4b. Although the runs in the temperature range 140−160 K have been extended to 80 million MC steps, calculated properties do not appear to be converged. Data collected from the first 40 million steps gave a similar irregular, apparently random, temperature dependence in this region. By comparing the solidlike regime below 120 K to the liquidlike regime at 200 K and above, the radius of gyration reveals that the cluster expands when the temperature increases above the melting point (Figure 4c). When going from 50 to 100 and 120 K, however, a peculiar decrease in K can be observed. This can be traced to a transition from its minimum configuration at 50 K, to a structure where the seven water molecules in the H-bonding network form a compact distorted cube with an $H_5O_2^+$ unit in one corner.

The probability density of having the proton at a certain distance from the CM of the cluster, P(CM-H^+), together with the oxygen−oxygen radial distribution function, g_{O-O}, are shown in Figure 5a-b for $T = 120$ and 200 K. The sharp peak in P(CM-H^+) at ∼3 Å for $T = 120$ K in Figure 5a is a result of the rigid structure, whereas at 200 K the water molecules are mobile enough to be found on "both sides" of the $H_5O_2^+$ unit, giving a smeared-out distribution. At temperatures in the range 140−160 K (not shown), the distribution P(CM-H^+) is similar to the one at 120 K, although somewhat broader. In this region, we can identify a behavior that is different from those at both lower and higher temperature. Although the temperature is clearly high enough to enable hydrogen bond breaking, and cause liquidlike behavior, we find that seven water molecules are confined with high probability on only one side of the $H_5O_2^+$ unit. The differences between the solidlike and

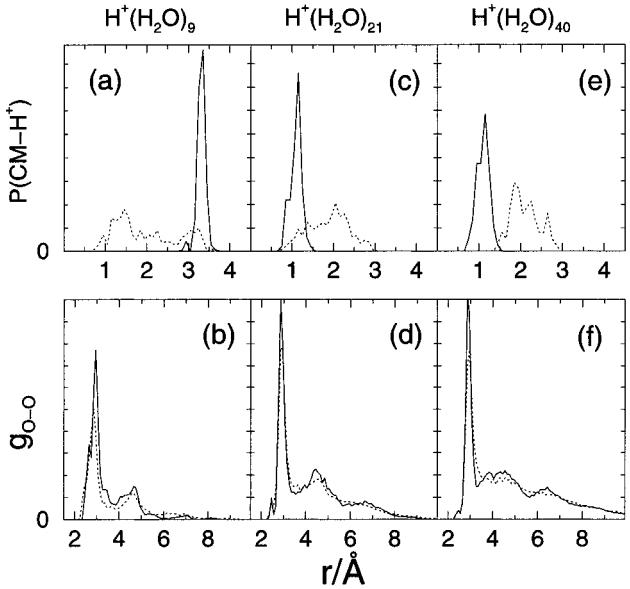

Figure 5. Probability density of having the proton at a certain distance from the center of mass (P(CM-H^+); upper panels), and the radial oxygen−oxygen distribution function (g_{O-O}, lower panels). The temperatures were (—) 120 and (···) 200 K for $H^+(H_2O)_9$ (panels a−b), (—) 150 and (···) 180 K for $H^+(H_2O)_{21}$ (panels c−d), and (—) 150 and (···) 250 K for $H^+(H_2O)_{40}$ (panels e−f).

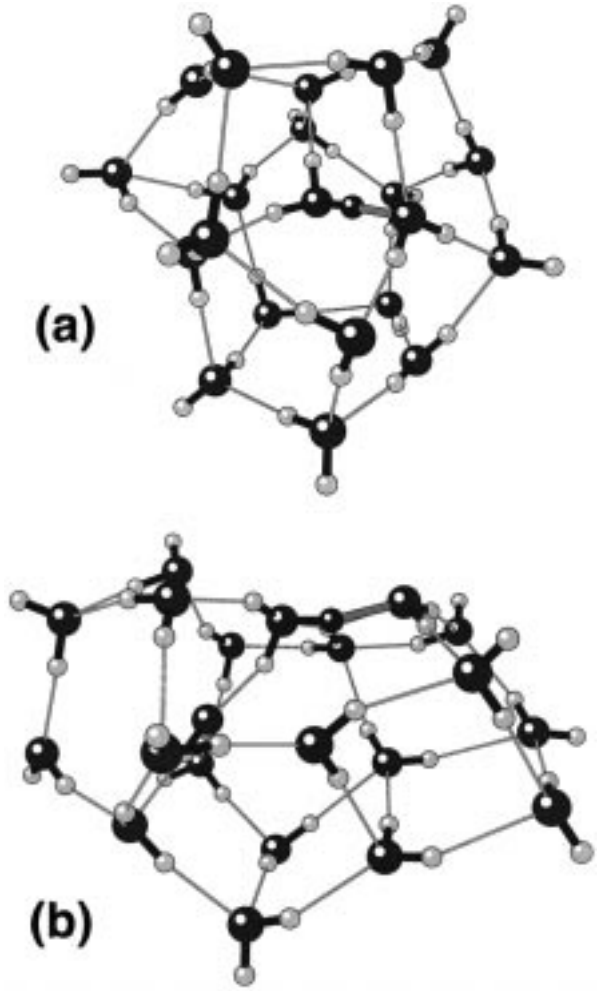

Figure 6. Lowest energy structure found for the $H^+(H_2O)_{21}$ cluster (panel a), together with a typical configuration at 180 K (panel b). Both covalent and hydrogen bonds are indicated and the proton is blackened.

liquidlike phases are less clearly reflected in g_{O-O} (Figure 5b), although a smoothening of the distribution is evident as the temperature is increased. A very similar behavior was found in the MD simulations of Berkowitz and co-workers[57,58] on $F^-(H_2O)_{11}$ and $Cl^-(H_2O)_{11}$ clusters. They applied the polarizable POL1 model and found "double-cube" minima with the F^- ion residing on the edge with four neighboring water molecules, and the Cl^- ion in one corner with three neighbors. When increasing the temperature from 0 to ~250 K, which is above the melting point, the coordination number increased from 4.0 to 5.1 and from 3.0 to 4.5 for the F^- and Cl^- ions, respectively. The distribution of cluster CM−ion distances also revealed an increased degree of solvation with increasing energy, due to entropic effects. In summary, the lowest energy structure of $H^+(H_2O)_9$ is predicted to have the ionic unit on the surface, and when the temperature reaches ~200 K, high-energy configurations can be accessed in which the ion moves closer to the center of the cluster.

The KJ model predicts a distorted dodecahedral cage as the minimum for $H^+(H_2O)_{21}$,[23] and the structure is shown in Figure 6a. Kozack and Jordan also found two disordered structures that were ~0.09 eV (2 kcal mol^{-1}) higher in energy. The temperature behavior is shown in Figures 4d−f, and we estimate T_m to be ~160 K. This value of T_m was confirmed by running microcanonical MD simulations at a few different energies, corresponding to cluster kinetic temperatures between 144 and 184 K. By comparing with $H^+(H_2O)_9$ we find that T_m is higher but also that the transition region is more narrow (Figure 4e). This result may be a consequence of the symmetric and ordered "filled-shell" structure of $H^+(H_2O)_{21}$ compared with the more disordered configuration of $H^+(H_2O)_9$. Note that similar differences were found with the neutral $(H_2O)_{20}$ clusters, where the transition from solidlike to liquidlike behavior was sharper for the pentagonal prism SPC cluster than for the cage-like KJ cluster. A further interesting feature is that despite the structural perturbation caused by the charged unit, the estimated melting temperatures of the $H^+(H_2O)_{21}$ and $(H_2O)_{20}$ (KJ) clusters, which are close in size, coincide. Analogous similarities were obtained by Berkowitz and co-workers[57] when comparing the melting characteristics of $F^-(H_2O)_{11}$, $Cl^-(H_2O)_{11}$, and $(H_2O)_{12}$ clusters, leading them to the conclusion that this process is mainly determined by water−water interactions.

Another sign of the melting transition can be traced in Figure 4f from the slope in K vs T, which is changing between 150 and 180 K. This is due to a severe structural change at 180 K, and a typical configuration at this temperature is displayed in Figure 6b. Above the melting point, the water molecules become mobile and the compact dodecahedron is destroyed. Although almost all hydrogen bonds were conserved at 150 K, only about one-fourth remained intact in the run at 180 K. The cluster also assumes a more elongated shape as seen in the increase in K_1 and K_2 together with a *decrease* in K_3 when going from 150 to 180 K. By examining Figure 5c, it is evident that the proton is always located close to the CM of the clusters at 150 K, whereas its distribution is broad at 180 K. The oxygen−oxygen radial distribution, displayed in Figure 5d, also broadens somewhat when the temperature is raised above the melting point. The small peak in g_{O-O} at ~2.5 Å, which is present for all three cluster sizes, is a result of the short oxygen−oxygen distance in the $H_5O_2^+$ unit.

It is instructive at this point to compare with the MD results of Smith and Dang[26] on $Cs^+(H_2O)_n$ clusters in the size range $n = 19-22$. Although they found a maximum in the incremental binding energies for $n = 20$ at 0 K, this effect was washed out for the liquidlike clusters at 220 K. They therefore concluded that the experimentally observed magic number behavior was either unobservable at higher temperatures or that it resulted from entropic effects in the liquidlike regime. Judging from our simulations, the dodecahedral cage structure of $H^+(H_2O)_{21}$ is a very unlikely configuration at temperatures above the melting point, and the connection between this structure and the magic number behavior should be restricted to low temperatures. This conclusion, together with the current prediction $T_m \approx 160$ K, is consistent with the fast flow tube experiments of Castleman and co-workers[15] performed at about 130 K. At temperatures >160 K and water partial pressures high enough to produce clusters of this size, experimental data are unfortunately not available, thus preventing a critical assessment. Further comparison with literature data can be done by calculating the difference in potential energy between the simulated $H^+(H_2O)_{21}$ and $H^+(H_2O)_9$ clusters. For the minimum energy structures this difference is quite large, 6.39 eV, but it decreases with temperature to 5.95 eV at 130 K, and to 4.49 eV at 300 K. Castleman et al.[14] measured decay fractions of $H^+(H_2O)_n$ clusters under vacuum conditions and calculated incremental binding energies in the size range $n = 6-28$. Although the temperature of the clusters is not known in these experiments, we would expect it to be in the vicinity of the freezing point.[59,60] By summing up the energies for the range $10 \le n \le 21$, we get 5.50 eV, which is quite close to the prediction of the KJ model

Figure 7. Lowest energy structure found for the $H^+(H_2O)_{40}$ cluster. Both covalent and hydrogen bonds are indicated and the proton is blackened.

at 130 K. The corresponding experimental data from Michl and co-workers[13] gives a substantially lower value, 3.31 eV, whereas Kelterbaum and Kochanski's MC simulations[2] at 300 K give 4.21 eV, which is in fair agreement with our data at this temperature.

We have also undertaken a limited series of simulations for $H^+(H_2O)_{40}$ clusters. Minimization was performed by several cycles of annealing followed by quenching from ~200 K, using three initial structures with different locations of the proton within the cluster. The most strongly bound structure we were able to produce had the charged unit near the center of the cluster, as shown in Figure 7, with a binding energy of 30.03 eV (Table 2). The binding energies of the alternative structures were only 0.2−0.3 eV lower. Figure 4g shows a low Lindemann index at 150 K and below, and the behavior is solidlike, with most of the H bonds being conserved throughout the simulations. At 250 and 300 K, the cluster is clearly in the liquidlike regime, as also revealed by the fact that essentially no H bonds survive the whole run. The increased flexibility is also visible in Figure 5e, where it is evident that at 150 K the proton resides close to the CM whereas at 250 K, the distribution is broader and shifted toward the surface of the cluster. Although the low-energy configurations for a cluster of this size most likely contain a well-hydrated charged unit close to the CM, the tendency for the charge to diffuse toward the surface at elevated temperature may well be due to an increase in entropy as a larger volume of configuration space is visited. A similar interpretation of the differences between the solidlike and liquidlike phases of $H^+(H_2O)_{21}$ seems plausible. The radius of the $H^+(H_2O)_{40}$ cluster, measured from the CM to the most distant molecule, is ~7 Å and it changes only weakly with temperature, which can also be inferred from the nearly constant radius of gyration in Figure 4i. By comparing E_p at 150 K with that of an alternative structure having the proton 4 Å from the center, we note that the difference is very small (<0.1 eV) compared with the thermal energy of the cluster. It is therefore likely that a number of alternative structures also exist in the solidlike regime.

Conclusions

In this study we have used an empirical polarizable water model to investigate the effect of temperature and size on the structure of protonated water clusters. The model predicts the melting temperature for $H^+(H_2O)_9$, $H^+(H_2O)_{21}$, and $(H_2O)_{20}$ to be ~130, ~160, and ~160 K, respectively. The agreement between the two latter temperatures indicates that the melting process is mainly governed by water−water interactions. Although the most stable configuration for the $H^+(H_2O)_9$ cluster exhibits an H-bonding network containing most water molecules and an ionic unit attached to the surface, the degree of solvation of this unit increases when the temperature reaches above the melting point. For the $H^+(H_2O)_{21}$ and $H^+(H_2O)_{40}$ clusters, on the other hand, the opposite trend is observed. The minimum for the $H^+(H_2O)_{21}$ cluster is a filled distorted dodecahedron with an H_3O^+-like unit close to the center. This ordered configuration is destroyed above the melting point, and the charged unit has a higher probability of residing closer to the surface. A similar conclusion applies to the $H^+(H_2O)_{40}$ cluster. Judging from the results presented in this article, proton hydrates present in the low-temperature mesopause region are most likely frozen. Even then, a range of solid structures may be present due to small differences in their binding energies.

Acknowledgment. This project was supported by the Swedish Natural Science Research Council.

References and Notes

(1) Lutrus, C. K.; Hagen, D. E.; Salk, S. H. S. *Atm. Environ. A* **1990**, *24*, 1397.
(2) Kelterbaum, R.; Kochanski, E. *J. Phys. Chem.* **1995**, *99*, 12493.
(3) Berry, R. S.; Beck, T. L.; Davis, H. L.; Jellinek, J. *Adv. Chem. Phys.* **1988**, *II*, 75, and references therein.
(4) Berry, R. S. *Chem. Rev.* **1993**, *93*, 2379, and references therein.
(5) Wales, D. J.; Doye, J. P. K. *J. Chem. Phys.* **1995**, *103*, 3061.
(6) Wales, D. J.; Ohmine, I. *J. Chem. Phys.* **1993**, *98*, 7245.
(7) Tsai, C. J.; Jordan, K. D. *J. Phys. Chem.* **1993**, *97*, 5208.
(8) Wales, D. J.; Ohmine, I. *J. Chem. Phys.* **1993**, *98*, 7257.
(9) Wales, D. J. *Science* **1996**, *271*, 925.
(10) Lin, S. S. *Rev. Sci. Instrum.* **1973**, *44*, 516.
(11) Echt, O.; Kreisle, D.; Knapp, M.; Recknagel, E. *Chem. Phys. Lett.* **1984**, *108*, 401.
(12) Nagashima, U.; Shinohara, H.; Nishi, N.; Tanaka, H. *J. Chem. Phys.* **1986**, *84*, 209.
(13) Magnera, T. F.; David, D. E.; Michl, J. *Chem. Phys. Lett.* **1991**, *182*, 363.
(14) Shi, Z.; Ford, J. V.; Wei, S.; Castleman, A. W., Jr. *J. Chem. Phys.* **1993**, *99*, 8009.
(15) Yang, X.; Castleman, A. W., Jr. *J. Geophys. Res. D* **1991**, *96*, 22573.
(16) Wei, S.; Shi, Z.; Castleman, A. W., Jr. *J. Chem. Phys.* **1991**, *94*, 3268.
(17) Shinohara, H.; Nagashima, U.; Tanaka, H.; Nishi, N. *J. Chem. Phys.* **1985**, *83*, 4183.
(18) Yang, X.; Castleman, A. W., Jr. *J. Phys. Chem.* **1990**, *94*, 8500.
(19) Steel, E. A.; Merz, K. M., Jr.; Selinger, A.; Castleman, A. W., Jr. *J. Phys. Chem.* **1995**, *99*, 7829.
(20) Buffey, I. P.; Byers Brown, W. *Chem. Phys. Lett.* **1984**, *109*, 59.
(21) David, C. W. *J. Mol. Struct.* **1987**, *150*, 391.
(22) Kelterbaum, R.; Kochanski, E. *J. Mol. Struct.* **1996**, *371*, 205.
(23) Kozack, R. E.; Jordan, P. C. *J. Chem. Phys.* **1993**, *99*, 2978.
(24) Kozack, R. E.; Jordan, P. C. *J. Chem. Phys.* **1992**, *96*, 3120.
(25) Kozack, R. E.; Jordan, P. C. *J. Chem. Phys.* **1992**, *96*, 3131.
(26) Smith, D. E.; Dang, L. X. *J. Chem. Phys.* **1994**, *101*, 7873.
(27) Xie, Y.; Remington, R. B.; Schaefer, H. F., III. *J. Chem. Phys.* **1994**, *101*, 4878.
(28) Ojamäe, L.; Shavitt, I.; Singer, S. J. *Int. J. Quantum Chem.* **1995**, *S29*, 657.
(29) Corongiu, G.; Kelterbaum, R.; Kochanski, E. *J. Phys. Chem.* **1995**, *99*, 8038.
(30) Gorb, L. G.; Ivashcenko, S. A.; Goncharuk, V. V. *J. Mol. Struct.* **1995**, *331*, 235.
(31) Khan, A. *Chem. Phys. Lett.* **1994**, *217*, 443.
(32) Laasonen, K.; Klein, M. L. *J. Phys. Chem.* **1994**, *98*, 10079.

(33) Tuckerman, M. E.; Ungar, P. J.; von Rosenvinge, T.; Klein, M. L. *J. Phys. Chem*. **1996**, *100*, 12878.
(34) Cheng, H.-P. *J. Chem. Phys.* **1996**, *105*, 6844.
(35) Sprik, M.; Hutter, J.; Parrinello, M. *J. Chem. Phys*. **1996**, *105*, 1142.
(36) Tuckerman, M. E.; Laasonen, K.; Sprik, M.; Parrinello, M. *J. Chem. Phys.* **1995**, *103*, 150.
(37) Björn, L. G.; Arnold, F. *Geophys. Res. Lett.* **1981**, *8*, 1167.
(38) Balsiger, F.; Kopp, E.; Friedrich, M.; Torkar, K. M.; Wälchli, U.; Witt, G. *Geophys. Res. Lett.* **1996**, *23*, 93.
(39) Witt, G. In *Space Research*, Vol. 4; Champion, K. S. W.; Smith, P. A.; Smith-Rose, R. L., Eds.; North-Holland: Amsterdam, 1969; p 157.
(40) Sugiyama, T. *J. Geophys. Res. A* **1994**, *99*, 3915.
(41) Allen, M. P.; Tildesley, D. J., *Computer Simulation of Liquids;* Clarendon: Oxford, 1990.
(42) Vesely, F. J. *J. Comput. Phys*. **1977**, *24*, 361.
(43) Jörgensen, W. L.; Chandrasekhar, J.; Madura, J. D.; Impey, R. W.; Klein M. L. *J. Chem. Phys*. **1983**, *79*, 926.
(44) Berendsen, H. J. C.; Postma, J. P. M.; van Gunsteren, W. F.; Hermans, J.; In *Intermolecular Forces*; Pullman, B.; Ed.; Reidel: Dordrecht, 1981; p 331.
(45) Dalleska, N. F.; Honma, K.; Armentrout, P. B. *J. Am. Chem. Soc*. **1993**, *115*, 12125.
(46) Eigen, M. *Angewandte Chemie* **1964**, *3*, 1.
(47) Svanberg, M.; Markovic', N.; Pettersson, J. B. C. *Chem. Phys.* **1995**, *201*, 473.
(48) Tsai, C. J.; Jordan, K. D. *J. Chem. Phys*. **1993**, *99*, 6957.
(49) Kirkpatrick, S.; Gelatt Jr., C. D.; Vecchi, M. P. *Science* **1983**, *220*, 671.
(50) Saito, S.; Ohmine, I. *J. Chem. Phys*. **1994**, *101*, 6063.
(51) Kinney, K. E.; Xu, S.; Bartell, L. S. *J. Phys. Chem*. **1996**, *100*, 6935.
(52) Grönbeck, H.; Tománek, D.; Kim, S.-G.; Rosén A. *Chem. Phys. Lett*. **1997**, *264*, 39.
(53) Sremaniak, L. S.; Perera, L.; Berkowitz, M. *J. Chem. Phys.* **1996**, *105*, 3715.
(54) Torchet, G.; Farges, J.; deFeuraudy, M. F.; Raoult, B. *Ann. Phys.* **1989**, *14*, 245.
(55) Huang, J.; Bartell, L. S. *J. Phys. Chem*. **1995**, *99*, 3924.
(56) Bixon, M.; Jortner, J. *J. Chem. Phys*. **1989**, *91*, 1631.
(57) Sremaniak, L. S.; Perera, L.; Berkowitz, M. *J. Phys. Chem.* **1996**, *100*, 1350.
(58) Perera, L.; Berkowitz, M. *J. Chem. Phys*. **1994**, *100*, 3085.
(59) Klots, C. E. *J. Chem. Phys.* **1985**, *83*, 5854.
(60) Klots, C. E. *Phys. Rev. A* **1989**, *39*, 339.